JNeurosci
THE JOURNAL OF NEUROSCIENCE

Research Articles: Cellular/Molecular

Direct interaction of PP2A phosphatase with $GABA_B$ receptors alters functional signaling

https://doi.org/10.1523/JNEUROSCI.2654-19.2020

Cite as: J. Neurosci 2020; 10.1523/JNEUROSCI.2654-19.2020

Received: 5 November 2019
Revised: 2 January 2020
Accepted: 18 February 2020

Direct interaction of PP2A phosphatase with $GABA_B$ receptors alters functional signaling

Xiaofan Li[1], Miho Terunuma[4], Tarek G. Deeb[2], Shari Wiseman[2], Menelas N. Pangalos[5], Angus C. Nairn[6], Stephen J. Moss[2,4 7] and Paul A. Slesinger[1,7]

[1]Nash Family Department of Neuroscience, Icahn School of Medicine at Mount Sinai, New York, NY 10029
[2]Department of Neuroscience, Tufts University School of Medicine, Boston MA 02111
[3]Department of Physiology, Pharmacology and Neuroscience, University College, London WC1E 6BT
[4]Division of Oral Biochemistry, Graduate School of Medical and Dental Sciences, Niigata University, Japan
[5]IMED Biotech Unit, AstraZeneca, Cambridge, United Kingdom
[6]Dept. Psychiatry, Yale University School of Medicine, New Haven, CT 065019
[7]Address correspondence to paul.slesinger@mssm.edu or Stephen.moss@tufts.edu

Key words: trafficking, phosphatase, GIRK channel, $GABA_B$ receptor, PP2A, PLA

Running title: PP2A / $GABA_B$ receptor complex

5 Figures
1 Table
Abstract word count: 192
Significance statement: 120
Introduction word count: 644
Discussion word count: 1113

Acknowledgements:
This work was supported in part by the National Institutes of Health (NIH)– National Institute on Drug Abuse (DA037170) for PAS and SJM, the National Institute on Alcohol Abuse and Alcoholism (AA018734) to PAS, the National Institute of Neurological Disorders and Stroke (NS051195, NS056359, NS081735, R21NS080064 and NS087662) for SJM, the National Institute of Mental Health (MH097446) for SJM, a 2017 NARSAD Young Investigator Grant to XL, and the Yale/NIDA Neuroproteomics Center (P30 DA018343) for SJM and ACN. We thank the Slesinger and Moss laboratories for discussions on the experiments.

Conflict of interest statement:
SJM serves as a consultant for AstraZeneca, and SAGE Therapeutics, relationships that are regulated by Tufts University. SJM holds stock in SAGE Therapeutics. No conflicts of interest for the other co-authors.

Abstract

Addictive drugs usurp the brain's intrinsic mechanism for reward, leading to compulsive and destructive behaviors. In the ventral tegmental area (VTA), the center of the brain's reward circuit, GABAergic neurons control the excitability of dopamine (DA) projection neurons and are the site of initial psychostimulant-dependent changes in signaling. Previous work established that cocaine/methamphetamine exposure increases protein phosphatase 2A (PP2A) activity, which dephosphorylates the $GABA_BR2$ subunit, promotes internalization of the $GABA_B$ receptor and leads to smaller $GABA_BR$-activated G protein-gated inwardly rectifying potassium (GIRK) currents in VTA GABA neurons. How the actions of PP2A become selective for a particular signaling pathway is poorly understood. Here, we demonstrate that PP2A can associate directly with a short peptide sequence in the C terminal domain of the $GABA_BR1$ subunit, and that $GABA_BRs$ and PP2A are in close proximity in rodent neurons (mouse/rat; mixed sexes). We show that this PP2A-$GABA_BR$ interaction can be regulated by intracellular Ca^{2+}. Finally, a peptide that potentially reduces recruitment of PP2A to $GABA_BRs$ and thereby limits receptor dephosphorylation increases the magnitude of baclofen-induced GIRK currents. Thus, limiting PP2A-dependent dephosphorylation of $GABA_BRs$ may be a useful strategy to increase receptor signaling for treating diseases.

Significance Statement:

Dysregulation of $GABA_B$ receptors underlie some of the altered neurotransmission in many neurological disorders. Protein phosphatase 2A (PP2A) is involved in dephosphorylating and subsequent internalization of $GABA_B$ receptors in models of addiction and depression. Here, we provide new evidence that PP2A B55 regulatory subunit interacts directly with a small region of the C-terminal domain of the $GABA_B$R1 subunit, and that this interaction is sensitive to intracellular Ca^{2+}. We demonstrate that a short peptide corresponding to the PP2A interaction site on $GABA_B$R1 competes for PP2A binding, enhances phosphorylation $GABA_B$R2 S783, and affects functional signaling through GIRK channels. Our study highlights how targeting PP2A dependent dephosphorylation of $GABA_B$Rs may provide a specific strategy to modulate $GABA_B$R signaling in disease conditions.

Introduction

$GABA_B$ receptors ($GABA_BRs$) are widely expressed in the nervous system and localized to extrasynaptic sites both pre- and post-synaptically. Activation $GABA_BRs$ dampens neuronal activity through several parallel pathways, including activation of G protein-gated inwardly rectifying potassium (GIRK) channels and inhibition of voltage-gated calcium channels and adenylyl cyclases. $GABA_BRs$ are obligatory heterodimers consisting of two structurally similar subunits, whereby the $GABA_BR1$ contains the ligand binding site, and $GABA_BR2$ contains binding sites for allosteric modulators and couples to G proteins (Galvez et al., 2000; Galvez et al., 2001). Surface expression of $GABA_BRs$ is determined by multiple tightly regulated trafficking processes, including ER export, internalization, recycling and degradation (Benke et al., 2012). Abnormal expression and signaling of $GABA_BRs$ has been associated with many psychiatric illnesses, including epilepsy, depression, anxiety and drug addiction (Bowery, 2006). Understanding the regulatory pathways of $GABA_BR$ trafficking will help us devise ways to remedy $GABA_BR$ signaling in disease conditions.

$GABA_BRs$ undergo agonist-induced desensitization, as well as cross-desensitization induced by activation of other receptors. Desensitization involves relatively fast processes at the level of G protein signaling and a slower process of receptor endocytosis (Raveh et al., 2015). $GABA_BRs$ are known to undergo constitutive endocytosis, followed by either degradation or recycling back to the plasma membrane (Vargas et al., 2008). How cells differentially regulate these pathways during receptor desensitization remains unclear. Unlike other GPCRs, $GABA_BR$ desensitization does not involve phosphorylation by G protein-coupled receptor kinases (GRKs). They are, however, phosphorylated by PKA, AMPK and CaMKII enzymes, with the former two stabilizing the receptor on the cell surface, and the latter promoting endocytosis and degradation (Couve et al., 2002; Kuramoto et al., 2007; Guetg et al., 2010a; Zemoura et al., 2019).

We previously demonstrated that the phosphorylation status of Serine 783 (S783) on $GABA_BR2$ determines receptor fate during post-endocytic sorting, whereby phosphorylation by AMPK promotes recycling, and dephosphorylation by protein phosphatase 2A (PP2A) leads to lysosomal degradation (Kuramoto et al., 2007; Terunuma et al., 2010). Importantly, AMPK and PP2A activities are ideally balanced at basal conditions. Ischemic injury or transient anoxia results in AMPK activation and enhance S783 phosphorylation on $GABA_BRs$, promoting $GABA_BR$ signaling and neuronal survival (Kuramoto et al., 2007). In cortical neurons, sustained NMDAR activation leads to a transient activation of AMPK and a corresponding transient increase in S783 phosphorylation/surface $GABA_BR$ expression, which is followed by a sustained decrease that is PP2A dependent (Terunuma et al., 2010). Whether PP2A directly dephosphorylates S783 is yet uncertain, but PP2A was pulled down by $GABA_BR1$ subunit (Terunuma et al., 2010), suggesting a possible direct interaction between the two.

PP2A-mediated regulation of $GABA_BR$-GIRK signaling has thus far been observed in multiple brain regions in response to various stimuli. A single dose of psychostimulants leads to sustained depression of $GABA_BR$-GIRK currents in VTA GABA neurons (Padgett et al., 2012). This effect can be abolished by acutely inhibiting PP2A, and is absent in mice with a S783A mutation (Padgett et al., 2012; Munoz et al., 2016), suggesting that PP2A exerts its influence by regulating S783 phosphorylation. Furthermore, in layer 5/6 pyramidal neurons of the prelimbic cortex, a PP2A-dependent suppression of $GABA_BR$-GIRK was observed following repeated cocaine exposure (Hearing et al., 2013). Acute foot shocks resulted in a decrease in $GABA_BR$-GIRK signaling in lateral habenula (LHb) neurons at 1 hour after the shock but persists for at least 2 weeks. PP2A inhibition rescued $GABA_BR$-GIRK currents as well as depressive-like behavioral phenotypes following foot shock stress (Lecca et al., 2016).

Together, these studies point to PP2A as a potential target for regulating aberrant $GABA_BR$ signaling. However, PP2A is a ubiquitous phosphatase with highly diversified families of B subunits (Sontag, 2001;

Slupe et al., 2011) and specific targeting of PP2A-$GABA_BR$ interaction remains an important puzzle to solve. In the current study, we examine how PP2A may be directed to the $GABA_BR$, and regulate phosphorylation of $GABA_BRs$ and their signaling through GIRK channels.

Materials and Methods

GST *pull-down experiments*

GST fusion proteins containing C-terminal deletions of the $GABA_BR1$ subunit were prepared as described previously (Couve et al., 2001). Adult male mice (C57BL6) were euthanized, brains were dissected and then homogenized in pull down assay buffer (50 mM Hepes-NaOH, pH 7.2, 5 mM $MgCl_2$, 150 mM NaCl, 10% Glycerol, 0.2% Triton X-100, 50 mM NaF, 10 mM sodium pyrophosphate, 1 mM sodium orthovanadate, 0.1% phenylmethylsulfonil fluoride, 10 μg/ml leupeptin, 10 μg/ml pepstatin A, 10 μg/ml antipain) using a sonicator. The homogenate was centrifuged at 150,000 rpm for 30 min at 4°C. 500 μg of supernatant was mixed with 20 μg of the corresponding fusion proteins immobilized on glutathione sepharose 4B beads (GE life sciences), and samples were rotated overnight at 4°C. Beads were washed twice in pull down assay buffer, twice in pull down assay buffer containing 500 mM NaCl, and twice in pull down assay buffer. Associated proteins were eluted in 40 μl of 2x sample buffer, separated by SDS-PAGE and transferred to nitrocellulose membrane for immunoblotting with antibodies for PP2A-B55 and PP2A-C. For pull-down, anti-PR55 (PP2A-B55) (clone 2G9; Upstate), anti-PP2Ac (BD Biosciences) and anti-$GABA_BR1$ (Santa Cruz Biotechnology) were used. All procedures and experiments using rodents were approved by the IACUC committees at Tufts and ISMMS.

Immunoprecipitation of native $GABA_B$ receptors in cultured cortical neurons

Cultured cortical neurons were prepared from E18 rat embryo as described previously (Terunuma et al., 2014) and were cultured in B27 containing Neurobasal media for 5 days at 37°C in a humidified

incubator with 5% CO_2. Neurons were then incubated with membrane-permeable TAT-R1-pep or scrambled peptides for 24 h at a concentration of 1 μM. Peptides were synthesized by New England peptide (www.newenglandpeptide.com) and were of >95% purity. The sequence of TAT-R1-pep was Biotin-GRKKRRQRRRPQGRQQLRSRRHPPT and TAT-scrambled was Biotin-GRKKRRQRRRPQGQPQRLRSPRHRT. Neurons were washed twice with PBS and lysed in Buffer A (20 mM Tris-HCl, pH 8.0, 150 mM NaCl, 5 mM EDTA, 1% Triton X-100, 10 mM NaF, 10 mM sodium pyrophosphate, 2 mM sodium orthovanadate, 0.1% phenylmethylsulfonil fluoride, 10 μg/ml leupeptin, 10 μg/ml pepstatin A, 10 μg/ml antipain). Homogenates were centrifuged at 150,000 rpm for 30 min at 4°C, preabsorbed with 40 μl of protein A agarose (Sigma) for 1 h at 4°C, and precleared supernatants were incubated with 1 μg of non-immune IgG or $GABA_BR1$ antibodies for 1hr at 4°C. Immune complexes were precipitated with 40 μl of protein A agarose overnight at 4°C, washed twice with Buffer A, twice with 500 mM NaCl containing Buffer A, and finally twice with Buffer A. Immunoprecipitated proteins were eluted in 40 μl of 2x sample buffer, boiled for 3min, and analyzed by SDS-PAGE followed by immunoblotting. For IP, anti-PR55 (PP2A-B55) (clone 2G9; Upstate), anti-PP2Ac (BD Biosciences), anti-$GABA_BR1$ (Santa Cruz Biotechnology), and anti-$GABA_BR2$ p783 (Kuramoto et al., 2007) were used.

Mass spectrometry analysis

$GABA_BR1$ antibody or IgG were crosslinked onto protein A beads using 0.2 M triethanolamine (pH 8.2) (TEA), in the presence of 40 mM dimethyl pimelimidate (DMP) at room temperature for 30 min. After extensive washing, immunoprecipitation was performed as detailed above with mouse cortical neurons. Precipitated material was separated by SDS-PAGE, stained with Coomassie and bands of interest were excised and digested with trypsin (Nakamura et al., 2016). Samples were then subject to LC-MS/MS at the Yale/NIDA Neuroproteomic Center (https://medicine.yale.edu/keck/nida/general/mission.aspx). MS/MS spectra were searched against the mouse database (Uniprot) using the Sequest 28 analysis

183 program. Peptide matches were considered true matches for ΔCN scores (delta correlation) > 0.2 and
184 XCorr values (cross correlation) greater than 2, 2, 3, 4 for +1, +2, +3, +4 charged peptides respectively
185 (Table 1). A particular protein would be considered present if at least five such high-quality peptides were
186 detected. Proteins in detergent solubilized extracts of cortical neurons that were purified on control IgG
187 were considered as non-specific.
188
189 *Cell culture and Proximity Ligation Assay (PLA)*
190 HEK293 cells were cultured in poly-D-lysine coated 12-well plates containing DMEM supplemented with
191 10% FBS, 1x Glutamax, 100 units/ml penicillin and 100 µg/ml streptomycin, at 37°C in a humidified air
192 incubator with 5% CO_2. Cells were transiently transfected using Lipofectamine 2000 with cDNA plasmids
193 expressing $GABA_BR1$-eYFP, $GABA_BR2$ and GIRK2a. 24 hours post transfection cells were trypsinized and
194 transferred to poly-D-lysine coated 8-well chamber slides and allowed to settle for 4-5 hours. Cells were
195 then fixed with 2% PFA in PBS for 7 minutes and permeabilized with PBS-0.1% Triton X for 5 minutes
196 before PLA assay.
197
198 For PLA with neurons, cerebral cortices of E18 C57B6/J mice were dissected in ice-cold HBSS
199 supplemented with 10mM HEPES and meninges were carefully removed. Cortical tissue was trimmed
200 into pieces and incubated with 0.25% trypsin at 37 °C for 15 minutes. Tissue was washed and triturated
201 in culture media (Neuralbasal Plus media supplemented with B-27 Plus, Glutamax and Pen-Strep; Gibco)
202 using fire-polished thin glass pipettes. Cells were filtered through a 40 µm nylon cell strainer, counted
203 and plated onto poly-D-lysine coated 8-well chamber slides (Falcon) at 5.7 x 10^5 cells/cm^2. Half media
204 exchanges were carried out every 2 days and 1 µM AraC was applied on DIV2 to inhibit non-neuronal
205 cell proliferation. PLA was carried out on DIV6.
206

PLA was performed using Duolink *in situ* reagents (Sigma-Aldrich) following the manufacturer's instructions. Anti-rabbit PLUS and anti-mouse MINUS PLA probes and red detection reagents were used. For cortical neurons, MAP2 immunostaining was carried out alongside PLA procedures. Slides were imaged with a digital camera (Canon) on a Zeiss fluorescence microscope with a 40x objective for HEK293 cells and 20x objective for cortical neurons. Exposure times, scope settings and lamp power were kept consistent for different experimental groups. PLA signals were quantified with particle analysis function in ImageJ after setting an appropriate threshold to filter out background signal. Cell numbers were counted manually. Antibodies used for PLA: anti-PP2A-C (Cell Signaling #2038), anti-PP2A-B55 (ThermoFisher MA5-15007), anti-$GABA_BR1$ (NeuroMab clone N93A/49), anti-$GABA_BR2$ (ThermoFisher PA5-23720), anti-MAP2 (Abcam ab5392).

Electrophysiology in Cultured Cortical Neurons

Rat cortical neurons were dissected as described above and plated onto glass coverslips at a density of 300,000 per 35 mm dish. Neurons were incubated in modified Neurobasal media (B27, Glutamax, glucose, Pen/Strep; ThermoFisher) for 18-21 days prior to recordings. Recordings were performed in a bath solution containing (in mM) 140 NaCl, 2.5 KCl, 2.5 $CaCl_2$, 2.5 $MgCl_2$, 10 HEPES, 11 glucose, pH 7.4 by NaOH. AP5 (50 μM), DNQX (20 μM), picrotoxin (100 μM) and TTX (500 nM) were added to the bath to block NMDA, AMPA, $GABA_A$ receptors and Na_V channels, respectively. Baclofen (10 μM) was used for $GABA_B$ receptor activation. The patch-pipette solution contained (in mM): 135 K-gluconate, 10 KCl, 2 disodium-ATP, 2 Mg-ATP, 0.4 Na-GTP, 10 HEPES, pH 7.4 by KOH. All reagents were purchased from Tocris Biosciences. The synthetic peptides were added directly to the patch-pipette solution at a working concentration of 50 μM. R1-pep contained amino acids RQQLRSRRHPPT and scrambled contained amino acids QPRTPRHLSQRR. Recordings were performed at a holding potential of -50 mV and at 34 °C. Series

resistance was monitored every 3 minutes to ensure that the recordings were stable over time. All data were acquired using an Axopatch 200B amplifier and pClamp software (Molecular Devices).

Experimental Design and Statistical Analyses

The design of experiments in this study involved either comparing two groups (e.g., PLA vs. one control, experimental vs. control peptide), or multiple groups (e.g., PLA vs. multiple controls). Sexes were mixed for all experiments, except for males used in GST pull-down experiments. For statistical analyses of two groups, we used a ratio-paired or unpaired Student's t-test (one or two-tailed). For statistical analyses of multiple groups, we used one-way ANOVA with Tukey post hoc test for significance (*P* value) between groups, with the significance indicated in the text. All calculations and comparisons were determined in Prism (GraphPad) and values reported as mean ± SEM, or in scatter plots with mean indicated by solid bar.

Results

PP2A is a trimeric protein consisting of a structural A subunit, a catalytic C subunit, and a regulatory B subunit (Sontag, 2001; Slupe et al., 2011). Previously, we found that the PP2A C subunit associates with the $GABA_BRs$ and specifically the $GABA_BR1$ subunit in a pull-down experiment with GST-$GABA_BR1$ (Terunuma et al., 2010). Here we confirmed this interaction by mass spec analysis of proteins immunoprecipitated from cortical neurons with $GABA_BR1$ antibody. We detected both the PP2A-Cα subunit and B55α subunit in precipitated material using the $GABA_BR1$ antibody, but not control IgG (**Table 1**). Next we sought to identify the amino acid sequences on $GABA_BR1$ that mediate this protein-protein interaction. To do so, we exposed the cytoplasmic domain of the R1 subunit (amino-acids 857-961) expressed as a glutathione-S-transferase fusion protein (GST-R1) to detergent solubilized brain extracts (**Figure 1A,B**). To assess recruitment of PP2A we immunoblotted GST pulldown material with an

antibody that recognizes the catalytic subunit (PP2A-C), a core component of this divergent family of phosphatases. PP2A-C was bound to GST-R1, but not to GST alone. The PP2A-B55 subunit was also detected, indicating binding to GST-R1 (**Figure 1C**). To further delineate which amino acid support binding to PP2A, we used shorter fusion proteins encoding distinct regions of $GABA_BR1$ subunit cytoplasmic domain $\Delta1$ - $\Delta6$ (**Figure 1B**). Compared to GST-R1, $\Delta1$ and $\Delta3$ exhibited reduced binding to PP2A-C and PP2A-B55 from brain lysates, while $\Delta4$ and $\Delta5$ showed little or no binding (**Figure 1 C,D**). Taken together, these results suggest that residues 917-927 are important in mediating the binding of $GABA_BR1$ to PP2A (**Figure 1B-D).** Consistent with this conclusion, $\Delta6$, which contains residues 905-928, was the smallest region that retained some interaction with PP2A.

To test whether the interaction between PP2A and $GABA_BR$ occurs in a living cell, we performed an *in situ* Proximity Ligation Assay (PLA) with HEK293 cells transfected with $GABA_BR1$ and $GABA_BR2$ subunits. PLA is a sensitive method that detects protein-protein interactions with single-molecule resolution (Weibrecht et al., 2010; Koos et al., 2014). The proximity of antibodies against two interacting proteins allows ligation of DNA strands conjugated to the antibodies, forming a circular DNA template. The circular DNA is then amplified by PCR, and detected by fluorescent DNA-binding probes (**Figure 2Ai**). Thus, each fluorescent puncta corresponds to one protein-protein complex. We first tested for interaction between endogenous PP2A and transiently expressed $GABA_BRs$ (**Figure 2A**). Antibodies against the PP2A catalytic subunit (PP2A-C) and $GABA_BR1$ C-terminus (R1) revealed a strong PLA signal (quantified as puncta per cell) in HEK293 cells transfected with $GABA_BR1$ and $GABA_BR2$ (**Figure 2Aiii**). eYFP fused to the $GABA_BR1$ subunit allowed detection of transfected cells. We also performed PLA in HEK293 cells co-transfected with GIRK2, a downstream effector of $GABA_BR$ that has been demonstrated to co-assemble with $GABA_BRs$ (Kulik et al., 2006; Fowler et al., 2007; Fernandez-Alacid et al., 2009; Ciruela et al., 2010). The presence of GIRK2, however, did not significantly increase the PLA signal between PP2A-C and $GABA_BR1$ (**Figure 2C**). For negative control, we performed two types of

experiments. In the first negative control, we omitted the primary antibody but used both PLA probes. For the second control, we omitted one secondary PLA probe. In both cases, we found significantly fewer puncta. (**Figure 2A-C**). The PLA signal was significantly smaller ($P < 0.0001$), and may represent background due to non-specific antibody/probe binding (**Figure 2A, iv-v; B & C**). In untransfected HEK cells, we also observed background levels of puncta (**Figure 2Avi & C**). HEK293 cells are reported to express $GABA_BR1$ but not $GABA_BR2$ mRNA (Atwood et al., 2011). Without $GABA_BR2$, however, $GABA_BR1$ cannot be trafficked to the cell surface and is trapped in the endoplasmic reticulum (ER) due to an ER retention signal present in the C-terminal domain (Couve et al., 1998; Margeta-Mitrovic et al., 2000; Pagano et al., 2001). Whether the weak PLA signal we observed in untransfected cells could come from native $GABA_BR1$ in the ER remains unknown.

Having shown a positive PLA signal with transfected HEK293 cells, we investigated whether the close association of PP2A with $GABA_B$ receptors also occurs with natively expressed proteins in neurons. We probed for interaction between $GABA_BR1$ and PP2A-C subunit, as well as between $GABA_BR1$ and the PP2A regulatory B55 subunit, in cultures of mouse cortical neurons. As a positive control for the PLA we tested for interaction between $GABA_BR1$ and $GABA_BR2$. We detected robust PLA signals for all three conditions, whereas very few puncta were seen with negative controls (one primary antibody omitted) (**Figure 3A-D**). The PLA signals were detected in both the soma and dendrites (marked by MAP2 immunostaining). The PLA signals quantified as puncta per cell were significantly higher than negative controls for association between PP2A-C subunit and $GABA_BR1$ ($P < 0.0001$), PP2A-B55α ($P < 0.0001$) and $GABA_BR1$ ($P < 0.0001$), as well as $GABA_BR1$ and $GABA_BR2$ subunits (**Figure 3D**).

Next, we examined whether the association between PP2A and $GABA_BR$ is physiologically regulated. We showed previously that increases in intracellular Ca^{2+} level, which models elevated neuronal activity, can enhance phosphorylation of S783 on $GABA_BR2$ (Terunuma et al., 2010). High Ca^{2+} level activates AMP-

dependent protein kinase (AMPK), which has been shown to phosphorylate S783 (Kuramoto et al., 2007; Terunuma et al., 2010). We hypothesized that under high Ca^{2+} level there is a concomitant decrease in PP2A-mediated dephosphorylation of S783 and potentially a decrease in the PP2A-$GABA_BR$ interaction. To test this hypothesis, we treated neurons with the calcium ionophore A23187 (2 μM) for 30 min, a condition that led to increased S783 phosphorylation in cortical neurons (Terunuma et al., 2010). In A23187-treated cells, we observed a significant decrease in the PLA signal for PP2A-C and $GABA_BR1$, as compared to vehicle-treated neurons (**Figure 3E-F**). Taken together, the PLA studies demonstrate that PP2A can associate with full-length $GABA_B$ receptors in different cell types, and that it is a dynamic interaction regulated by intracellular Ca^{2+}.

If the direct association of PP2A with the $GABA_B$ receptor is important for dephosphorylating p-S783, then we hypothesized that a R1 peptide that competes for PP2A binding might reduce the dephosphorylation, and therefore increase p-S783 (Terunuma et al., 2010). To test this hypothesis, we designed a new R1 peptide (TAT-R1-pep) that contains a TAT sequence (Green and Loewenstein, 1988) for crossing the plasma membrane and examined the effect in cultures of cortical neurons. TAT-R1-pep which competes for binding of PP2A to native $GABA_BR1$ reduced the amount of both PP2A B and C subunits that associates with $GABA_BR1$ in co-immunoprecipitation experiments (**Figure 4A**). In addition, TAT-R1-pep significantly increased the level of S783 phosphorylation on the R2 subunit suggesting that interaction of PP2A with the C-terminus of $GABA_BR1$ helps to regulate the phosphorylation state of S783 in $GABA_BR2$ (**Figure 1A**).

Previous work established that PP2A-dependent dephosphorylation of p-S783 controls surface expression of $GABA_B$ receptors in neurons (Terunuma et al., 2010). To examine if exposure to the $GABA_BR1$ peptide affects $GABA_B$ receptor function, we measured the rate of current rundown, a phenomenon inherent to whole-cell recordings that is caused by the dialysis of the intracellular milieu

and results in the rapid internalization of specific membrane proteins (Kuramoto et al., 2007). Application of baclofen (10 μM) leads to stimulation of $GABA_B$ receptors, which in turn activate the GIRK channels. Baclofen activated an outward current that quickly began to rundown over the course of the 15 min recording (**Figure 5Ai**). In cells exposed to the scrambled control peptide, the percentage of current remaining at the end of the recording period was 48 ± 4 % (N = 7 neurons) (**Figure 5A-C**). By contrast, cells exposed to the R1-pep peptide retained 71 ± 5 % (N = 7 neurons) of the baseline current (**Figure 5Aii**), which was significantly greater than the control peptide (p = 0.0046, two-tailed unpaired t-test) (**Figure 5B, C**). In the absence of baclofen, the change in the holding current during the 15 minute recording was small and not significantly different with each peptide (10.2 ± 2.9 pA for scrambled, vs 11.7 ± 4.9 pA for R1 peptide, P = 0.7958, unpaired t-test). This result suggested there was no non-specific effect of R1 peptide on membrane currents in the cortical neurons. Taken together, these data support the conclusion that the physical interaction between the $GABA_B$ receptor and PP2A plays a direct role in the internalization of $GABA_B$ receptors (Terunuma et al., 2010).

Discussion

In this study, we provide evidence that PP2A associates directly with the $GABA_B$ receptor, through a specific series of amino acids located in the C-terminal domain of the $GABA_B$R1 subunit. Disruption of this $GABA_B$R1/PP2A interaction appears to reduce dephosphorylation of p-S783 on the $GABA_B$R2 subunit, and promote surface expression and functional coupling to GIRK channels in cortical neurons. We discuss the implications of these findings in the context of subcellular signaling and neurological diseases.

PP2A diversity and specificity

Mice injected with psychostimulants exhibit smaller $GABA_B$R-activated GIRK currents in VTA GABA neurons, which is expected to increase neuronal excitability of GABA neurons (Padgett et al., 2012;

Rifkin et al., 2018). We showed previously that this downregulation of $GABA_B$ receptors was due to PP2A-dependent dephosphorylation of p-S783 and internalization of the $GABA_B$ receptor (Padgett et al., 2012). Subsequently, the same PP2A-dependent downregulation of $GABA_B$ receptor function was also reported in mPFC and lateral habenula neurons, in response to cocaine and foot shock, respectively (Hearing et al., 2013; Lecca et al., 2016). Similarly, Maeda et al. reported that a PP2A inhibitor suppressed restraint-induced hyperlocomotion in cocaine-sensitized mice (Maeda et al., 2006). Thus, PP2A is emerging as a putative therapeutic target for treating addiction. The challenge, however, is that PP2A is a ubiquitous phosphatase in the body. PP2A is a heterotrimeric complex comprised of three subunits, a catalytic (C), a scaffold (A) and a regulatory (B) subunit (Slupe et al., 2011). Different B subunits provide substrate specificity for PP2A, with the B subunit determining whether PP2A is found in the nucleus, cytosol or attached to the cytoskeleton (Sontag, 2001; Slupe et al., 2011). How the actions of PP2A become selective for a particular signaling pathway is of great interest but poorly understood. Here, we provide new evidence that PP2A associates directly with the $GABA_B$ receptor. First, PP2A containing the B55α subunit (see Table 1) co-precipitates with $GABA_B$ receptors and binds to a small region of the $GABA_B$R1 C terminal domain. Second, $GABA_B$ receptors expressed either in HEK293 cells or natively in neurons are positioned within a few nm of PP2A, as indicated by a positive PLA signal (Weibrecht et al., 2010; Koos et al., 2014). What promotes the interaction of PP2A with the $GABA_B$ receptor? In the striatum, activation of D1Rs leads to increase in cAMP and PKA activation, which in turn phosphorylates PP2A and ultimately leads to dephosphorylation of p-T75 on DARPP-32 (Ahn et al., 2007a; Ahn et al., 2007b). The mechanism underlying the increase in PP2A activity with psychostimulants in VTA GABA neurons, however, remains unknown. Experiments suggest elevations in intracellular Ca^{2+}, either through NMDA receptor activation or a Ca^{2+} ionophore, can regulate the interaction of PP2A with the $GABA_B$ receptor. We found that increase in intracellular Ca^{2+} via the Ca^{2+} ionophore A23187, leads to a decrease in association of PP2A with the $GABA_B$ receptors (decrease in

371 PLA signal). This would correspond to the initial increase in p-S783 seen with A23187 (Terunuma et al.,
372 2010).
373
374 In addition to the PP2A-dependent pathway, $GABA_B$ receptor trafficking is also influenced by
375 Ca^{2+}/Calmodulin-dependent protein kinase II (CaMKII). NMDA-dependent internalization of $GABA_B$
376 receptors also occurs via activation of CaMKII and phosphorylation of serine 867 (S867) in the C terminal
377 domain of $GABA_B$R1 subunit (Guetg et al., 2010b). PKA-dependent phosphorylation of S892 on $GABA_B$R2
378 promotes stabilization of the receptor on the plasma membrane (Fairfax et al., 2004) and KCTD12 was
379 recently shown to enhance phosphorylation of S892 (Adelfinger et al., 2014). The interplay of regulatory
380 proteins like PP2A and the balance of phosphorylation provide a complex and dynamic mechanism in
381 regulating the surface expression of $GABA_B$ receptors in neurons.
382
383 *Binding site and Complex formation*
384 The PP2A binding site on $GABA_B$R1 was narrowed to the region containing $_{918}$RQQLRSRRHPPT$_{929}$, which is
385 adjacent to the coiled-coil domain of $GABA_B$R1 that is involved in dimerization with the $GABA_B$R2 subunit
386 (White et al., 1998; Kammerer et al., 1999; Margeta-Mitrovic et al., 2000; Burmakina et al., 2014). The
387 finding that PP2A associates directly with $GABA_B$ receptors provides further support for a $GABA_B$
388 receptor signaling complex that contains a multitude of regulatory proteins. In addition, the $GABA_B$
389 receptor can associate with GIRK channels in a signaling complex (Kulik et al., 2006; Fowler et al., 2007;
390 Fernandez-Alacid et al., 2009; Ciruela et al., 2010). GIRK channels can also directly associate with
391 trafficking proteins, such as SNX27 (Lunn et al., 2007; Balana et al., 2011). Indeed, a cluster of proteins
392 has been identified that interact directly with, or close to, $GABA_B$ receptors (this study & (Schwenk et al.,
393 2016)). How these protein-protein interactions are regulated and what is the functional impact remain
394 important questions to be addressed in the future. While the evidence is clear that PP2A associates

with and regulates $GABA_B$ receptors in the brain, this association could occur either at the plasma membrane or within intracellular compartments. Although we provide evidence that B55 containing PP2A interacts with $GABA_BR1$, whether it is the B55 subunit that mediates the direct binding and whether other families of B subunits could mediate PP2A-$GABA_BR1$ interaction remain to be tested.

Tat peptide strategy and disease

PP2A inhibitors have been used successfully in animal models to treat anxiety- and depression-like phenotypes (Lecca et al., 2016; Tchenio et al., 2017; O'Connor et al., 2018). In humans, PP2A inhibitors have been used as chemo-sensitizers in treating cancer (O'Connor et al., 2018). For example, LB-100 is a small molecule inhibitor of the PP2A-C subunit and has been tested in Phase I clinical trials for treating solid tumors in combination with Docetaxel (O'Connor et al., 2018). However, there are unwanted side-effects with these broad spectrum PP2A inhibitors. Developing a more targeted approach, such as specifically interfering with the association of PP2A with its target as described in our study (i.e., $GABA_B$ receptor) could provide a more efficacious and specific strategy for treating human neurological diseases. The ability of TAT peptides to cross cell membranes makes them an ideal tool for this purpose. We showed that a TAT-R1 peptide can significantly reduce dephosphorylation of $GABA_B$ receptors and affect $GABA_B$-GIRK signaling. It will be of interest in the future to determine if slow synaptic transmission mediated by $GABA_B$ receptors and GIRK channels is also affected by antagonizing the interaction of PP2A with $GABA_BRs$. TAT peptides have been used to inhibit β-adrenergic receptor activation of I_f (Saponaro et al., 2018), to disrupt GluA2 association with GAPDH *in vivo*, protecting against epilepsy-induced neuronal damage (Zhang et al., 2018), and for interfering with NR2B association with Src, decreasing NR2B tyrosine phosphorylation (Ba et al., 2019). Recently, a TAT-modified w-conotoxin peptide was shown to cross the blood-brain-barrier, providing some analgesia (Yu et al., 2019). Thus, TAT peptides offer a promising option for treatment of brain disorders.

References

Adelfinger L, Turecek R, Ivankova K, Jensen AA, Moss SJ, Gassmann M, Bettler B (2014) GABAB receptor phosphorylation regulates KCTD12-induced K(+) current desensitization. Biochem Pharmacol 91:369-379.

Ahn J-H, McAvoy T, Rakhilin SV, Nishi A, Greengard P, Nairn AC (2007a) Protein kinase A activates protein phosphatase 2A by phosphorylation of the B56 subunit. Proceedings of the National Academy of Sciences 104:2979-2984.

Ahn J-H, Sung JY, McAvoy T, Nishi A, Janssens V, Goris J, Greengard P, Nairn AC (2007b) The B''/PR72 subunit mediates Ca2+-dependent dephosphorylation of DARPP-32 by protein phosphatase 2A. Proceedings of the National Academy of Sciences 104:9876-9881.

Atwood BK, Lopez J, Wager-Miller J, Mackie K, Straiker A (2011) Expression of G protein-coupled receptors and related proteins in HEK293, AtT20, BV2, and N18 cell lines as revealed by microarray analysis. BMC Genomics 12:14.

Ba M, Yu G, Yang H, Wang Y, Yu L, Kong M (2019) Tat-Src reduced NR2B tyrosine phosphorylation and its interaction with NR2B in levodopa-induced dyskinetic rats model. Behav Brain Res 356:41-45.

Balana B, Maslennikov I, Kwiatkowski W, Stern KM, Bahima L, Choe S, Slesinger PA (2011) Mechanism underlying selective regulation of G protein-gated inwardly rectifying potassium channels by the psychostimulant-sensitive sorting nexin 27. Proc Natl Acad Sci USA 108:5831-5836.

Benke D, Zemoura K, Maier PJ (2012) Modulation of cell surface GABA(B) receptors by desensitization, trafficking and regulated degradation. World J Biol Chem 3:61-72.

Bowery NG (2006) GABAB receptor: a site of therapeutic benefit. Curr Opin Pharmacol 6:37-43.

Burmakina S, Geng Y, Chen Y, Fan QR (2014) Heterodimeric coiled-coil interactions of human GABAB receptor. Proc Natl Acad Sci USA 111:6958-6963.

442 Ciruela F, Fernández-Dueñas V, Sahlholm K, Fernández-Alacid L, Nicolau JC, Watanabe M, Luján R (2010)
443 Evidence for oligomerization between GABAB receptors and GIRK channels containing the GIRK1
444 and GIRK3 subunits. Eur J Neurosci:no-no.
445 Couve A, Filippov AK, Connolly CN, Bettler B, Brown DA, Moss SJ (1998) Intracellular retention of
446 recombinant GABAB receptors. J Biol Chem 273:26361-26367.
447 Couve A, Kittler JT, Uren JM, Calver AR, Pangalos MN, Walsh FS, Moss SJ (2001) Association of GABA(B)
448 receptors and members of the 14-3-3 family of signaling proteins. Mol Cell Neurosci 17:317-328.
449 Couve A, Thomas P, Calver AR, Hirst WD, Pangalos MN, Walsh FS, Smart TG, Moss SJ (2002) Cyclic AMP-
450 dependent protein kinase phosphorylation facilitates GABA(B) receptor-effector coupling. Nat
451 Neurosci 5:415-424.
452 Fairfax BP, Pitcher JA, Scott MGH, Calver AR, Pangalos MN, Moss SJ, Couve A (2004) Phosphorylation and
453 Chronic Agonist Treatment Atypically Modulate GABAB Receptor Cell Surface Stability. J Biol
454 Chem 279:12565-12573.
455 Fernandez-Alacid L, Aguado C, Ciruela F, Martin R, Colon J, Cabanero MJ, Gassmann M, Watanabe M,
456 Shigemoto R, Wickman K, Bettler B, Sanchez-Prieto J, Lujan R (2009) Subcellular compartment-
457 specific molecular diversity of pre- and post-synaptic GABA-activated GIRK channels in Purkinje
458 cells. J Neurochem 110:1363-1376.
459 Fowler CE, Aryal P, Suen KF, Slesinger PA (2007) Evidence for association of $GABA_B$ receptors with Kir3
460 channels and RGS4 proteins. J Physiol 580:51-65.
461 Galvez T, Duthey B, Kniazeff J, Blahos J, Rovelli G, Bettler B, Prezeau L, Pin JP (2001) Allosteric
462 interactions between GB1 and GB2 subunits are required for optimal GABA(B) receptor function.
463 EMBO J 20:2152-2159.

464 Galvez T, Prezeau L, Milioti G, Franek M, Joly C, Froestl W, Bettler B, Bertrand HO, Blahos J, Pin JP (2000)
465 Mapping the agonist-binding site of GABAB type 1 subunit sheds light on the activation process
466 of GABAB receptors. J Biol Chem 275:41166-41174.
467 Green M, Loewenstein PM (1988) Autonomous functional domains of chemically synthesized human
468 immunodeficiency virus tat trans-activator protein. Cell 55:1179-1188.
469 Guetg N, Abdel Aziz S, Holbro N, Turecek R, Rose T, Seddik R, Gassmann M, Moes S, Jenoe P, Oertner TG,
470 Casanova E, Bettler B (2010a) NMDA receptor-dependent GABAB receptor internalization via
471 CaMKII phosphorylation of serine 867 in GABAB1. Proc Natl Acad Sci U S A 107:13924-13929.
472 Guetg N, Aziz SA, Holbro N, Turecek R, Rose T, Seddik R, Gassmann M, Moes S, Jenoe P, Oertner TG,
473 Casanova E, Bettler B (2010b) NMDA receptor-dependent GABAB receptor internalization via
474 CaMKII phosphorylation of serine 867 in GABAB1. Proceedings of the National Academy of
475 Sciences 107:13924-13929.
476 Hearing M, Kotecki L, Marron Fernandez de Velasco E, Fajardo-Serrano A, Chung HJ, Lujan R, Wickman K
477 (2013) Repeated cocaine weakens GABA(B)-Girk signaling in layer 5/6 pyramidal neurons in the
478 prelimbic cortex. Neuron 80:159-170.
479 Kammerer RA, Frank S, Schulthess T, Landwehr R, Lustig A, Engel J (1999) Heterodimerization of a
480 functional GABAB receptor is mediated by parallel coiled-coil alpha-helices. Biochemistry
481 38:13263-13269.
482 Koos B, Andersson L, Clausson C-m, Grannas K, Klaesson A, Cane G, Söderberg O (2014) Analysis of
483 protein interactions in situ by proximity ligation assays. Current topics in microbiology and
484 immunology 377:111-126.
485 Kulik A, Vida I, Fukazawa Y, Guetg N, Kasugai Y, Marker CL, Rigato F, Bettler B, Wickman K, Frotscher M,
486 Shigemoto R (2006) Compartment-dependent colocalization of Kir3.2-containing K^+ channels
487 and $GABA_B$ receptors in hippocampal pyramidal vells. J Neurosci 26:4289-4297.

488 Kuramoto N, Wilkins ME, Fairfax BP, Revilla-Sanchez R, Terunuma M, Tamaki K, Iemata M, Warren N,
489 Couve A, Calver A, Horvath Z, Freeman K, Carling D, Huang L, Gonzales C, Cooper E, Smart TG,
490 Pangalos MN, Moss SJ (2007) Phospho-dependent functional modulation of GABA(B) receptors
491 by the metabolic sensor AMP-dependent protein kinase. Neuron 53:233-247.
492 Lecca S, Pelosi A, Tchenio A, Moutkine I, Lujan R, Herve D, Mameli M (2016) Rescue of GABAB and GIRK
493 function in the lateral habenula by protein phosphatase 2A inhibition ameliorates depression-
494 like phenotypes in mice. Nat Med 22:254-261.
495 Lunn M-L, Nassirpour R, Arrabit C, Tan J, McLeod I, Arias CM, Sawchenko PE, Yates JR, Slesinger PA
496 (2007) A unique sorting nexin regulates trafficking of potassium channels via a PDZ domain
497 interaction. Nat Neurosci 10:1249-1259.
498 Maeda T, Yoshimatsu T, Hamabe W, Fukazawa Y, Kumamoto K, Ozaki M, Kishioka S (2006) Involvement
499 of serine/threonine protein phosphatases sensitive to okadaic acid in restraint stress-induced
500 hyperlocomotion in cocaine-sensitized mice. Brit J Pharmacol 148:405-412.
501 Margeta-Mitrovic M, Jan YN, Jan LY (2000) A trafficking checkpoint controls GABA(B) receptor
502 heterodimerization. Neuron 27:97-106.
503 Munoz MB, Padgett CL, Rifkin R, Terunuma M, Wickman K, Contet C, Moss SJ, Slesinger PA (2016) A Role
504 for the GIRK3 Subunit in Methamphetamine-Induced Attenuation of GABAB Receptor-Activated
505 GIRK Currents in VTA Dopamine Neurons. J Neurosci 36:3106-3114.
506 Nakamura Y, Morrow DH, Modgil A, Huyghe D, Deeb TZ, Lumb MJ, Davies PA, Moss SJ (2016) Proteomic
507 Characterization of Inhibitory Synapses Using a Novel pHluorin-tagged gamma-Aminobutyric
508 Acid Receptor, Type A (GABAA), alpha2 Subunit Knock-in Mouse. J Biol Chem 291:12394-12407.
509 O'Connor CM, Perl A, Leonard D, Sangodkar J, Narla G (2018) Therapeutic targeting of PP2A.
510 International Journal of Biochemistry and Cell Biology 96:182-193.

511 Padgett CL, Lalive AL, Tan KR, Terunuma M, Munoz MB, Pangalos MN, Martinez-Hernandez J, Watanabe
512 M, Moss SJ, Lujan R, Luscher C, Slesinger PA (2012) Methamphetamine-evoked depression of
513 GABA(B) receptor signaling in GABA neurons of the VTA. Neuron 73:978-989.
514 Pagano A, Rovelli G, Mosbacher J, Lohmann T, Duthey B, Stauffer D, Ristig D, Schuler V, Meigel I,
515 Lampert C, Stein T, Prezeau L, Blahos J, Pin J, Froestl W, Kuhn R, Heid J, Kaupmann K, Bettler B
516 (2001) C-terminal interaction is essential for surface trafficking but not for heteromeric
517 assembly of GABA(b) receptors. J Neurosci 21:1189-1202.
518 Raveh A, Turecek R, Bettler B (2015) Mechanisms of fast desensitization of GABA(B) receptor-gated
519 currents. Adv Pharmacol 73:145-165.
520 Rifkin RA, Huyghe D, Li X, Parakala M, Aisenberg E, Moss SJ, Slesinger PA (2018) GIRK currents in VTA
521 dopamine neurons control the sensitivity of mice to cocaine-induced locomotor sensitization.
522 Proc Natl Acad Sci USA 115:E9479-E9488.
523 Saponaro A, Cantini F, Porro A, Bucchi A, Difrancesco D, Maione V, Donadoni C, Introini B, Mesirca P,
524 Mangoni ME, Thiel G, Banci L, Santoro B, Moroni A (2018) A synthetic peptide that prevents
525 camp regulation in mammalian hyperpolarization-activated cyclic nucleotide-gated (HCN)
526 channels. eLife 7:1-22.
527 Schwenk J, Perez-Garci E, Schneider A, Kollewe A, Gauthier-Kemper A, Fritzius T, Raveh A, Dinamarca
528 MC, Hanuschkin A, Bildl W, Klingauf J, Gassmann M, Schulte U, Bettler B, Fakler B (2016)
529 Modular composition and dynamics of native GABAB receptors identified by high-resolution
530 proteomics. Nat Neurosci 19:233-242.
531 Slupe AM, Merrill Ra, Strack S (2011) Determinants for Substrate Specificity of Protein Phosphatase 2A.
532 Enzyme research 2011:398751.
533 Sontag E (2001) Protein phosphatase 2A: the Trojan Horse of cellular signaling. Cell Signal 13:7-16.

534 Tchenio A, Lecca S, Valentinova K, Mameli M (2017) Limiting habenular hyperactivity ameliorates
535 maternal separation-driven depressive-like symptoms. Nat Commun 8:1135.
536 Terunuma M, Vargas KJ, Wilkins ME, Ramirez OA, Jaureguiberry-Bravo M, Pangalos MN, Smart TG, Moss
537 SJ, Couve A (2010) Prolonged activation of NMDA receptors promotes dephosphorylation and
538 alters postendocytic sorting of GABAB receptors. Proc Natl Acad Sci U S A 107:13918-13923.
539 Terunuma M, Revilla-Sanchez R, Quadros IM, Deng Q, Deeb TZ, Lumb M, Sicinski P, Haydon PG, Pangalos
540 MN, Moss SJ (2014) Postsynaptic GABAB receptor activity regulates excitatory neuronal
541 architecture and spatial memory. J Neurosci 34:804-816.
542 Vargas KJ, Terunuma M, Tello JA, Pangalos MN, Moss SJ, Couve A (2008) The availability of surface GABA
543 B receptors is independent of gamma-aminobutyric acid but controlled by glutamate in central
544 neurons. J Biol Chem 283:24641-24648.
545 Weibrecht I, Leuchowius KJ, Clausson CM, Conze T, Jarvius M, Howell WM, Kamali-Moghaddam M,
546 Soderberg O (2010) Proximity ligation assays: a recent addition to the proteomics toolbox.
547 Expert Rev Proteomics 7:401-409.
548 White JH, Wise A, Main MJ, Green A, Fraser NJ, Disney GH, Barnes AA, Emson P, Foord SM, Marshall FH
549 (1998) Heterodimerization is required for the formation of a functional $GABA_B$ receptor. Nature
550 396:679-682.
551 Yu S, Li Y, Chen J, Zhang Y, Tao X, Dai Q, Wang Y, Li S, Dong M (2019) TAT-Modified ω-Conotoxin MVIIA
552 for Crossing the Blood-Brain Barrier. Marine drugs 17.
553 Zemoura K, Balakrishnan K, Grampp T, Benke D (2019) Ca(2+)/Calmodulin-Dependent Protein Kinase II
554 (CaMKII) beta-Dependent Phosphorylation of GABAB1 Triggers Lysosomal Degradation of
555 GABAB Receptors via Mind Bomb-2 (MIB2)-Mediated Lys-63-Linked Ubiquitination. Mol
556 Neurobiol 56:1293-1309.

557 Zhang J, Qiao N, Ding X, Wang J (2018) Disruption of the GluA2/GAPDH complex using TAT-GluA2 NT1-3-
558 2 peptide protects against AMPAR-mediated excitotoxicity after epilepsy. NeuroReport 29:432-
559 439.

Figure legends

Figure 1. Identification of the PP2A binding site in $GABA_BR1$ C-terminal domain. **A**, Cartoon shows binding of PP2A (consisting of A, B and C subunits) to the C-terminal domain of the $GABA_BR1$ subunit. **B**, Schematic of seven different GST-tagged C terminal $GABA_BR1$ constructs used to localize the region of R1 involved in binding to PP2A. Numbers indicate amino acid positions in the full-length $GABA_BR1$ subunit. **C**, Immunoblot of pull-down. $GABA_BR1$ fusion proteins or GST alone were exposed to mouse brain lysates and bound proteins were subject to immunoblotting with antibodies against B55 (PR55), and C subunits of PP2A. Control lane shows input of PP2A enzyme. Bottom picture shows equal loading of GST fusion proteins revealed by Coomassie blue staining. **D**, Bar chart shows the levels of PP2A binding to the different $GABA_BR1$ fusion proteins determined after subtracting background binding to GST alone. Mean ± SEM is shown for three separate experiments.

Figure 2. Interaction between PP2A and $GABA_BR$ full-length proteins as detected by proximity ligation assay (PLA) in HEK293 cells. **A**, i, Schematic of the PLA reaction between PP2A (antibody against C subunit) and eYFP-tagged $GABA_BR$ (antibody against $GABA_BR1$ C-terminus). ii-vi, Representative PLA images of HEK293 cells for the indicated experimental conditions: HEK293 cells were transfected with the cDNAs indicated above each image, and primary antibodies used for PLA are indicated (bottom left). Green: eYFP signal indicating transfected cells. Red: PLA signal; each red puncta represents a single PP2A-$GABA_BR$ complex. Blue: DAPI staining. **B**, Scatter plot shows quantification of PLA signal from one representative experiment. Each data point represents analysis of one image containing 1-11 HEK cells. Presence or absence of primary antibodies and secondary probes (m, mouse; r, rabbit) are indicated below. Magenta bar indicates mean. ****$P<0.0001$, one-way ANOVA with Tukey post hoc test ($F(5, 53) = 70.76$). **C**, Scatter plot of normalized PLA signal pooled from three independent experiments. Data

583 points were normalized to the R1+R2+GIRK2a PLA condition (1st column). UT, untransfected. Magenta
584 bar indicates mean. ****P<0.0001, one-way ANOVA with Tukey post hoc test (F (6, 182) = 134.5).
585
586 **Figure 3. Evidence for interaction of endogenous PP2A and $GABA_BR$ in cultured cortical neurons**. **A-C**,
587 Representative PLA images of cultured mouse cortical neurons (DIV 6) with the indicated primary
588 antibodies. Top 3 panels (i) show PLA signal (red) between PP2A-C subunit and $GABA_BR1$, PP2A-B55 and
589 $GABA_BR1$, and between $GABA_BR1$ and $GABA_BR2$ subunits. Bottom 3 panels (ii) show corresponding
590 negative controls where a primary antibody was omitted. Green: MAP2 immunostaining. Red: PLA
591 signal. Blue: DAPI staining. **D**, Scatter plot shows quantification of PLA signal corresponding to A-C from
592 one representative experiment. Each data point represents analysis of one image containing ~80
593 neurons. Magenta bar indicates mean. ****P<0.0001 using unpaired Student's two-tailed t-test. **E-F**,
594 Regulation of PP2A-C and $GABA_BR1$ interaction by intracellular Ca^{2+}. **E**, Representative images of DIV 6
595 cortical neurons treated with vehicle (i) or the calcium ionophore A23187 (2 µM, ii) for 30 min before
596 PLA for PP2A-C and $GABA_BR1$. **F**, Scatter plot shows normalized PLA signal pooled from three
597 independent experiments. Data points were normalized to the vehicle average for each experiment.
598 Control group received vehicle treatment but PP2A-C antibody was omitted. Red bar indicates group
599 mean for three experiments. ****p<0.0001, one-way ANOVA with Tukey post hoc test (F (2, 81) =
600 167.8).
601
602 **Figure 4. PP2A binding to $GABA_BR1$ modulates level of phosphorylation at S783 in $GABA_BR2$ subunit.**
603 **A**, Co-immunoprecipitation (co-IP) of $GABA_BR1$ and PP2A from cultured rat neurons treated with
604 membrane permeant TAT-R1-pep or TAT-scrambled peptides. Total lysates (input) shown on the left.
605 Note decrease in PP2A B55 and C subunits with TAT-R1-pep. Bar graph shows the quantification of co-IP
606 (PP2A-B55/R1 ratio) for TAT-R1-pep condition normalized to the TAT-scrambled peptide. Note

significant decrease in PP2A with TAT-R1-pep. Mean ± SEM shown with individual points (*P = 0.0122; t=4.214, df=3; one-tailed ratio paired t-test). Asterisk for IgG control indicates non-specific signal with secondary antibody. Arrowhead indicates size for $GABA_BR1$. **B**, Increase in phosphorylation of S783 in $GABA_BR2$ subunit after TAT-R1-pep treatment. Blot shows Western with antibody recognizing phosphorylated S783 in R2 (p-S783) for scrambled (TAT-scramb) and TAT-R1-pep conditions following immunoprecipitation of the R1 subunit. Ponceau S shows total protein following IP. **C**, Bar graph shows the quantification of p-S783 phosphorylation for TAT-R1-pep condition normalized to the TAT-scrambled peptide. Note significant increase in phosphorylation with TAT-R1-pep (*P= 0.0266; t=4.157, df=2, one-tailed ratio paired t-test).

Figure 5. R1-pep peptide attenuates rundown of baclofen-activated GIRK currents ($I_{Baclofen}$) in cultured cortical neurons. **A**, Representative traces showing baclofen-activated currents recorded from rat cortical neurons at baseline (0 min) and after 15 min for the scrambled peptide (i) (QPRTPRHLSQRR, black traces) and PP2A-interfering peptide (ii) (R1-pep: RQQLRSRRHPPT, magenta traces). Black bars above traces indicate the duration of the baclofen (10 μM) pulse. Holding potential was -50 mV. *Inset*, cartoon shows inclusion of peptides in the patch pipette and thus directly exposed to the cell interior**. B**, Plot of the normalized $I_{Baclofen}$ over time for recordings with control peptide (scrambled, black) and R1-pep peptide (magenta). Mean ± SEM shown (N= 7 cells per condition). **C**, Dot plot shows the current remaining at 15 min expressed as a percentage of the baclofen-induced current at 0 min for cells exposed to either R1-pep (magenta) or scrambled peptide (black). Bar indicates mean. **P=0.0046; t=3.468, df=12, two-tailed unpaired t-test.

Table 1. Proteins immunoprecipitated with $GABA_BRs$ from cultured cortical neurons. Mass spectrometry analysis of proteins immunoprecipitated with antibodies against $GABA_BR1$ or IgG from

mouse cortical neurons. Samples were digested with trypsin and subjected to LC-MS/MS to identify proteins precipitated with $GABA_BR1$ antibodies. The percentage coverage of each target protein is shown. The experimental data represent mean of two samples analyzed in parallel (duplicates). Note detection of PP2A-Cα (PP2AA) and PP2A-B55α (2ABA) subunits.

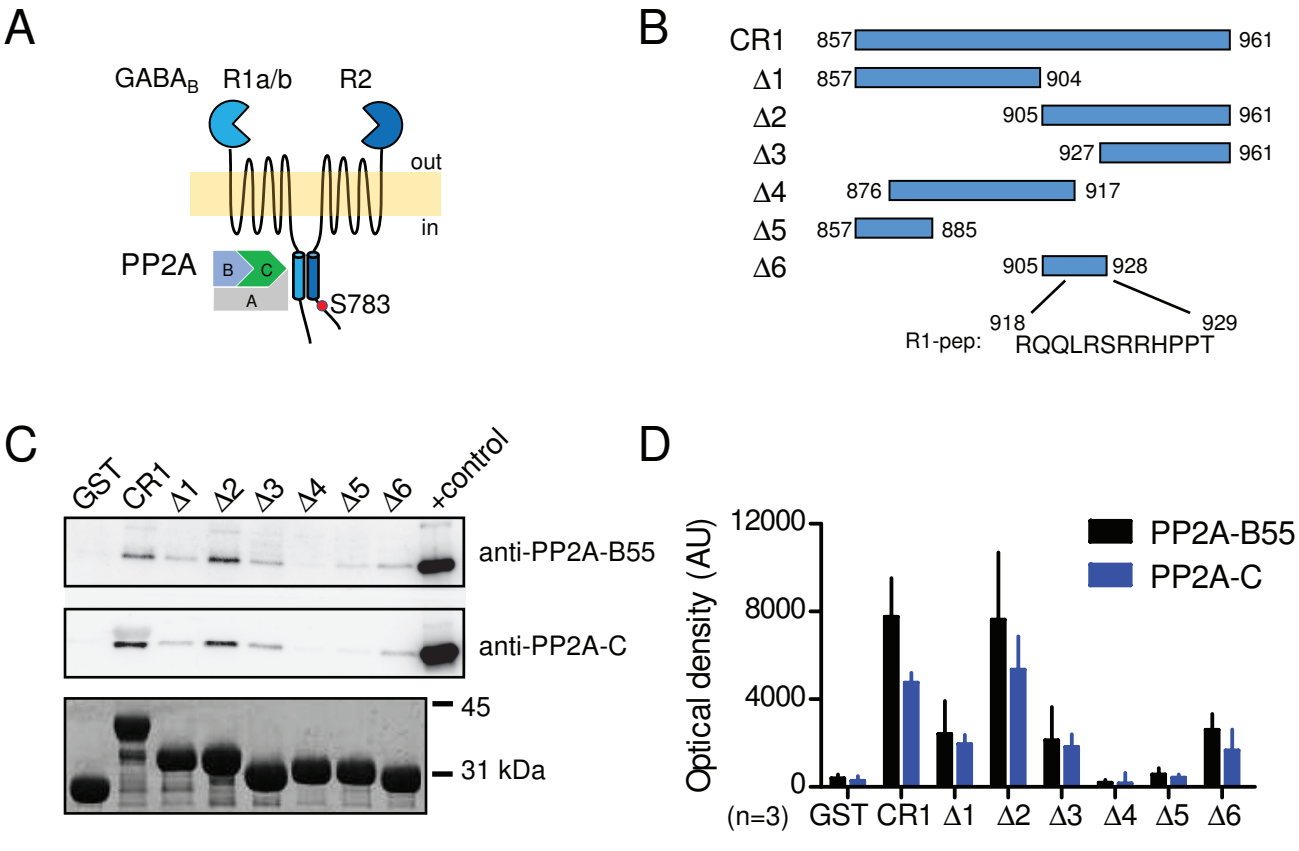

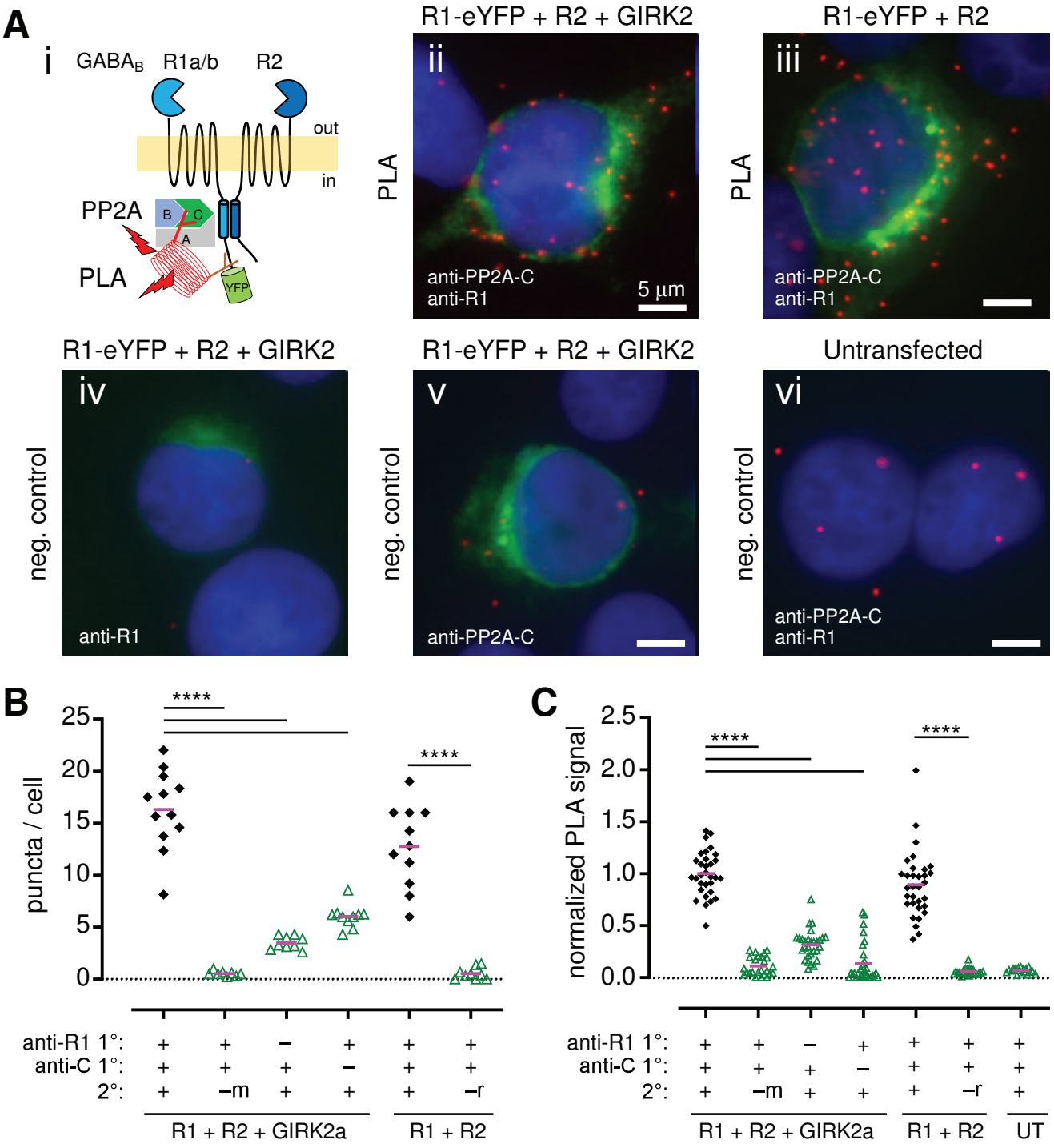

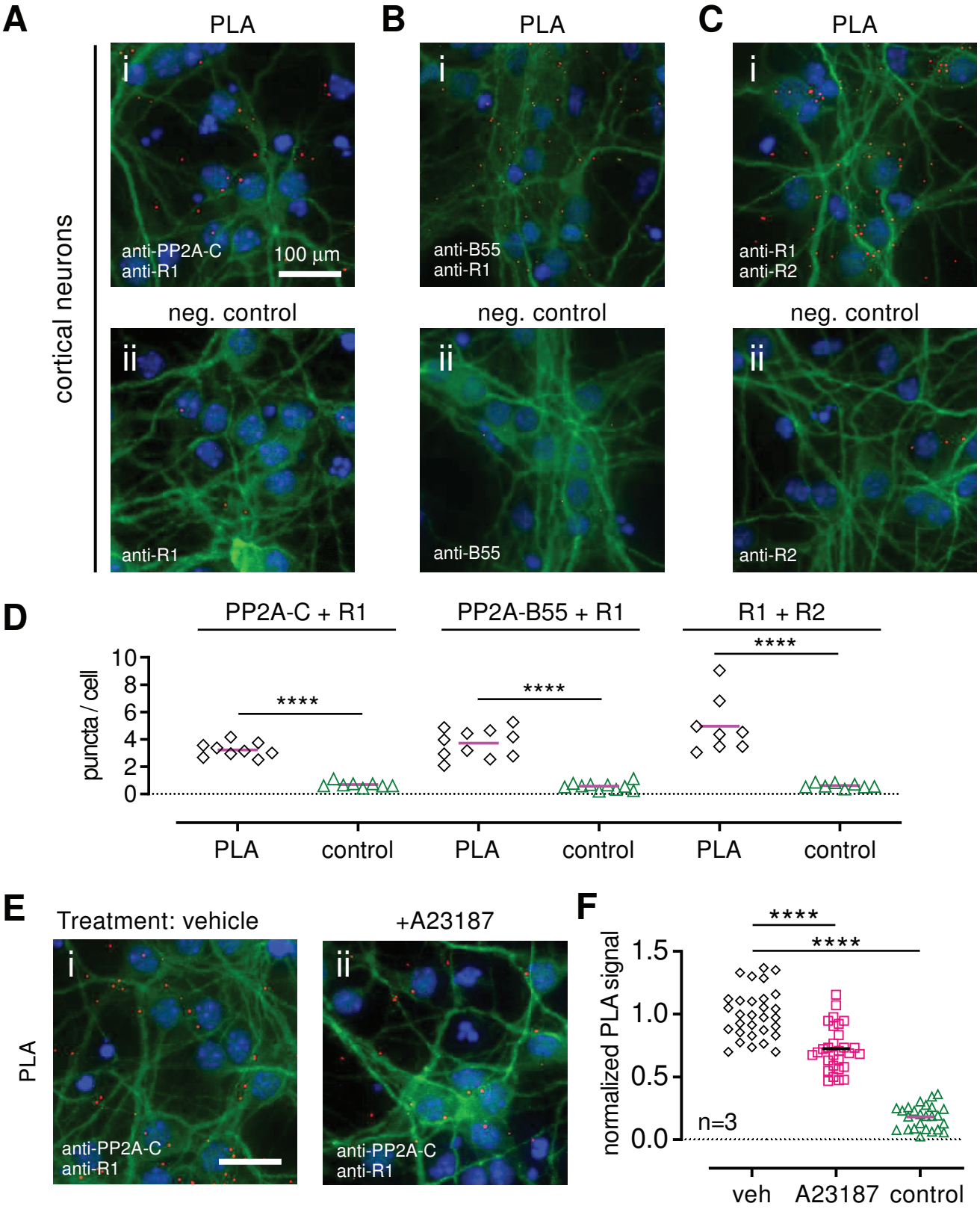

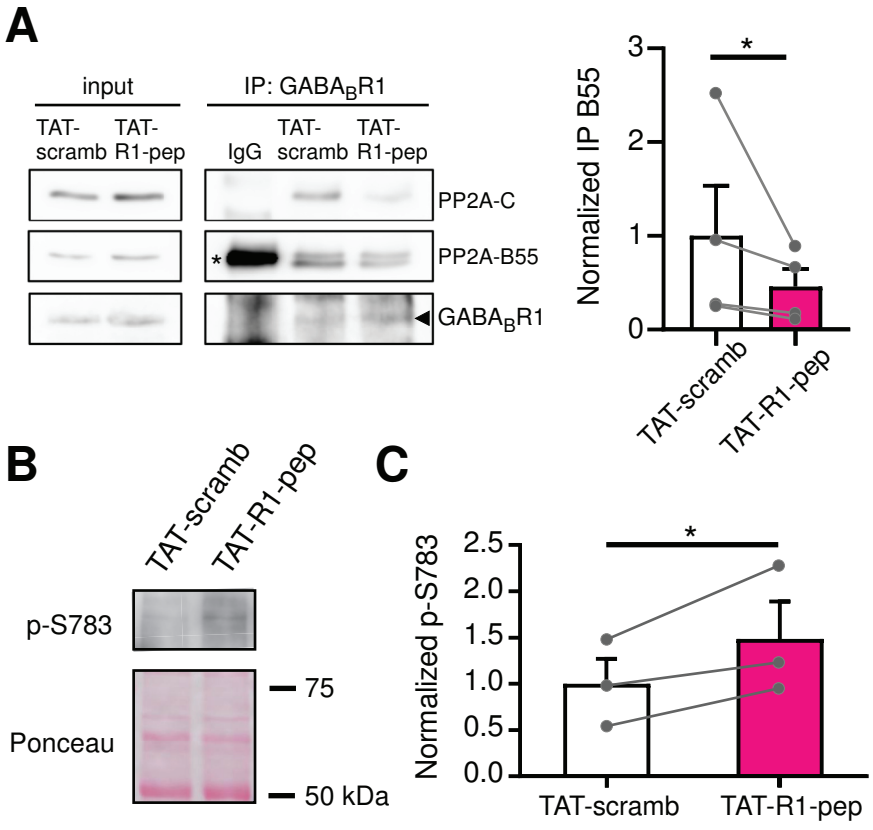

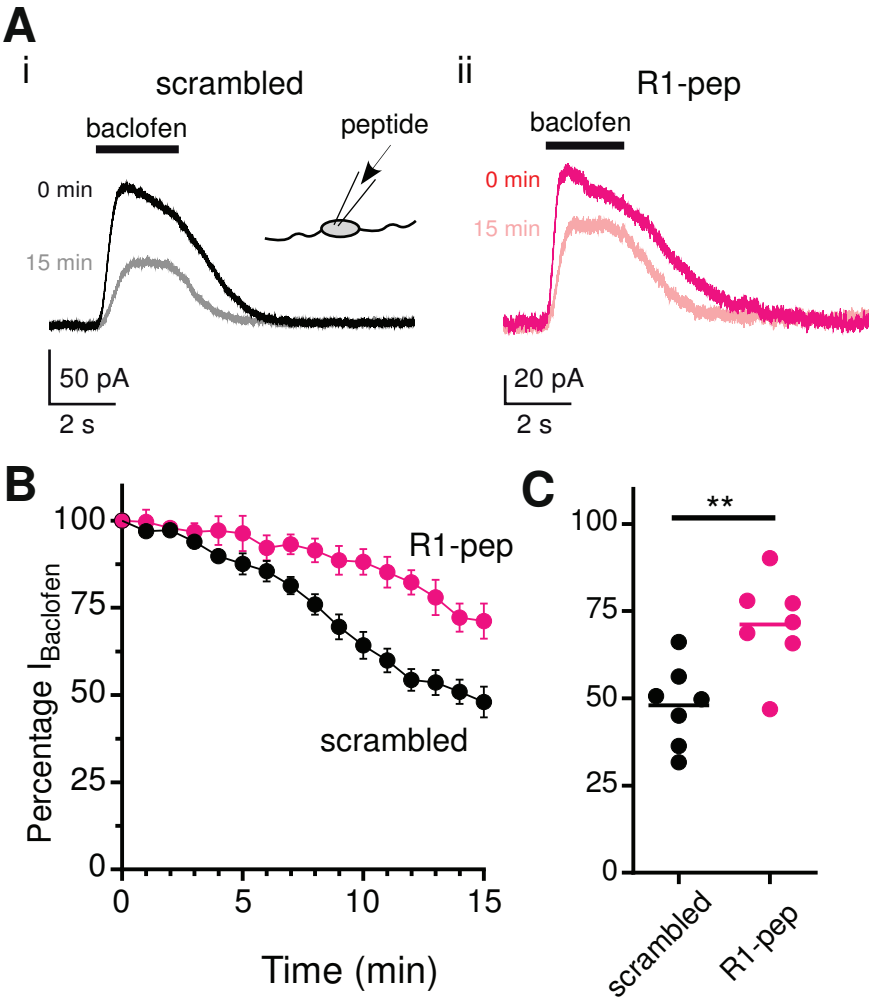

Table 1 – Analysis of $GABA_BR1$ associated proteins

Protein ID	Protein Name	IgG_% Coverage	R1 % Coverage
USMG5	Up-regulated during skeletal muscle growth protein	0	25.9
RL39	60S ribosomal protein L39	0	19.6
RL37A	60S ribosomal protein L37a	0	14.7
CNRP1	CB1 cannabinoid receptor-interacting protein 1	0	9.8
PROF1	Profilin-1 OS=Mus musculus	0	8.6
GDIR1	Rho GDP-dissociation inhibitor 1	0	7.8
RS26	40S ribosomal protein S26	0	7.8
RS15A	40S ribosomal protein S15a	0	6.9
DPYL1	Dihydropyrimidinase-related protein 1	0	7.25
RL27A	60S ribosomal protein L27a	0	6.8
H10	Histone H1.0	0	6.7
COF1	Cofilin-1 OS=	0	6.6
KV5A5	Ig kappa chain V-V region T1	0	8.95
RAB2A	Ras-related protein Rab-2A	0	6.1
RAP2A	Ras-related protein Rap-2a	0	6
CANB1	Calcineurin subunit B type 1	0	5.9
OTUB1	Ubiquitin thioesterase OTUB1	0	5.5
RS16	40S ribosomal protein S16	0	5.5
RL9	60S ribosomal protein L9	0	5.2
RL11	60S ribosomal protein L11	0	6.5
RAB5A	Ras-related protein Rab-5A	0	5.1
NDUS3	NADH dehydrogenase [ubiquinone] iron-sulfur protein 3, mitochondrial	0	4.9
TPM3	Tropomyosin alpha-3 chain	0	4.6
PGAM1	Phosphoglycerate mutase 1	0	5.7
RL7	60S ribosomal protein L7	0	4.1
HNRPD	Heterogeneous nuclear ribonucleoprotein D0	0	3.9
PP2AA	Serine/threonine-protein phosphatase 2A catalytic subunit alpha isoform	0	3.6
ERLN1	Erlin-1	0	3.5
SC6A1	Sodium- and chloride-dependent GABA transporter 1	0	3.5
EF1G	Elongation factor 1-gamma	0	3
SFXN5	Sideroflexin-5	0	2.9
SERA	D-3-phosphoglycerate dehydrogenase	0	2.8
2ABA	Serine/threonine-protein phosphatase 2A 55 kDa regulatory subunit B alpha isoform	0	2.7
ROA3	Heterogeneous nuclear ribonucleoprotein A3	0	2.6
NDUAA	NADH dehydrogenase [ubiquinone] 1 alpha subcomplex subunit 10, mitochondrial	0	2.5
GUAD	Guanine deaminase	0	2.5
Sep-05	Septin-5	0	2.4
NPTN	Neuroplastin	0	2.65
Sep-03	Neuronal-specific septin-3	0	2.3
ARP3	Actin-related protein 3	0	2.2
PFKAM	ATP-dependent 6-phosphofructokinase, muscle type	0	1.6
TCPG	T-complex protein 1 subunit gamma	0	2